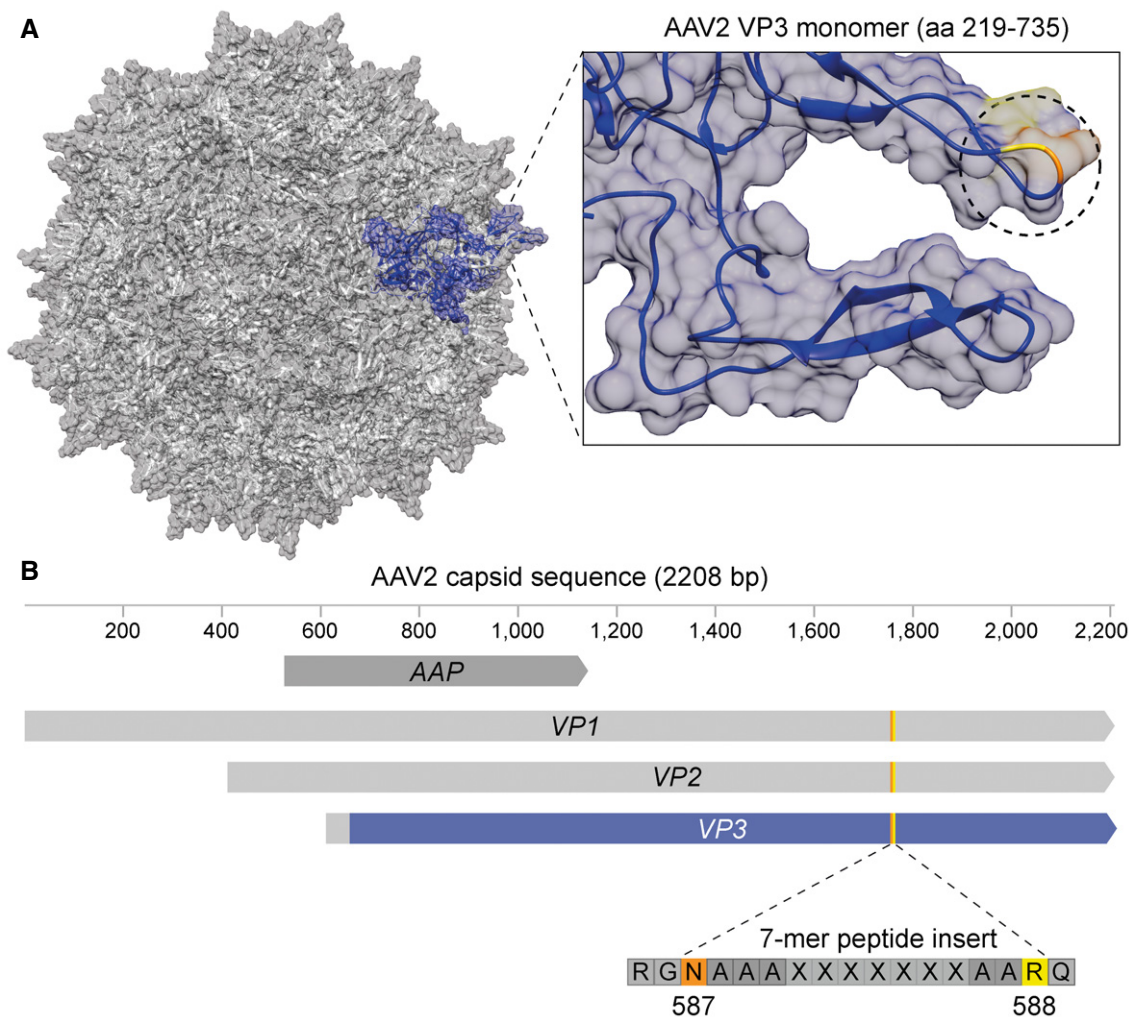
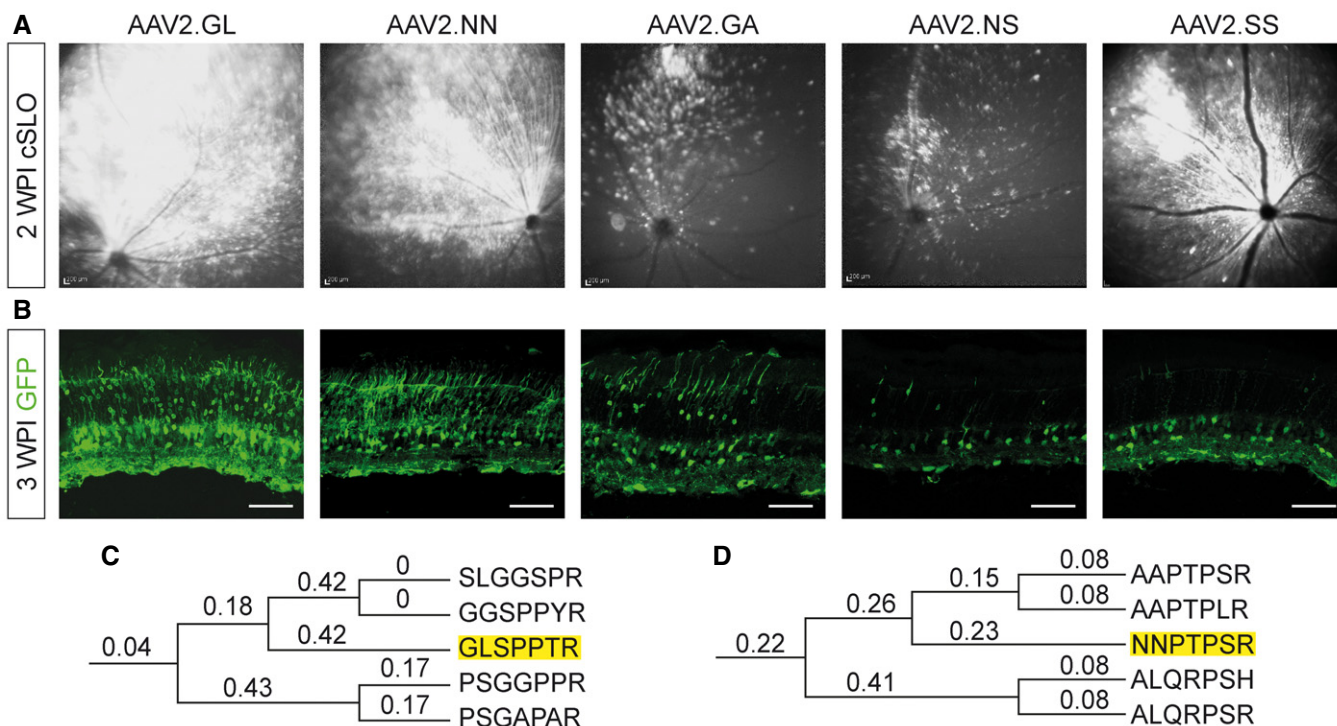


## Expanded View Figures

**Figure EV1. Schematic summary of peptide-display capsid diversification strategy.**

A Depiction of the parental AAV2 capsid structure (PDB 6IH9) with a single VP3 monomer (amino acids (aa) 219–735) coloured blue. On the right, the blue monomer is shown in focus and the unmodified insertion position I-587 is circled with the residues N587 and R588 highlighted in orange and yellow, respectively.

B Schematic of AAV2 capsid sequence with the constituent genes, i.e. assembly activating protein (AAP) and viral protein (VP) 1–3. The part of VP3—coloured blue represents the sequence of the structural monomer depicted in (A) with the same colour. The orange/yellow line in VP3 and schematic below indicate the site of insertion of the random 7-mer peptides between N587 (orange) and R588 (yellow) flanked by alanine linkers.



**Figure EV2. Selection of optimal candidate from vectorised rAAV variants.**

Comparative study between vectorised novel capsid variants AAV2.GL, AAV2.NN, AAV2.GA, AAV2.NS and AAV2.SS packaged with sc-CMV-eGFP; intravitreal administration of 2E9 vg.

A cSLO reporting transduction and spread of vectors in the murine retina after 2 WPI.

B Confocal scans of native eGFP fluorescence after 3WPI. Scale bar: 50  $\mu$ m. Acquisition settings were kept constant for all samples. GFP = eGFP.

C, D Phylogenetic tree of a selection of AAV variants detected via NGS in the cone (C) and rod (D) DNA from screening round 3. The amino acid sequences of peptide inserts were aligned, and a phylogenetic tree was constructed using the maximum likelihood method. Numbers indicate bootstrap values, and the peptides corresponding to AAV2.GL and AAV2.NN are highlighted.

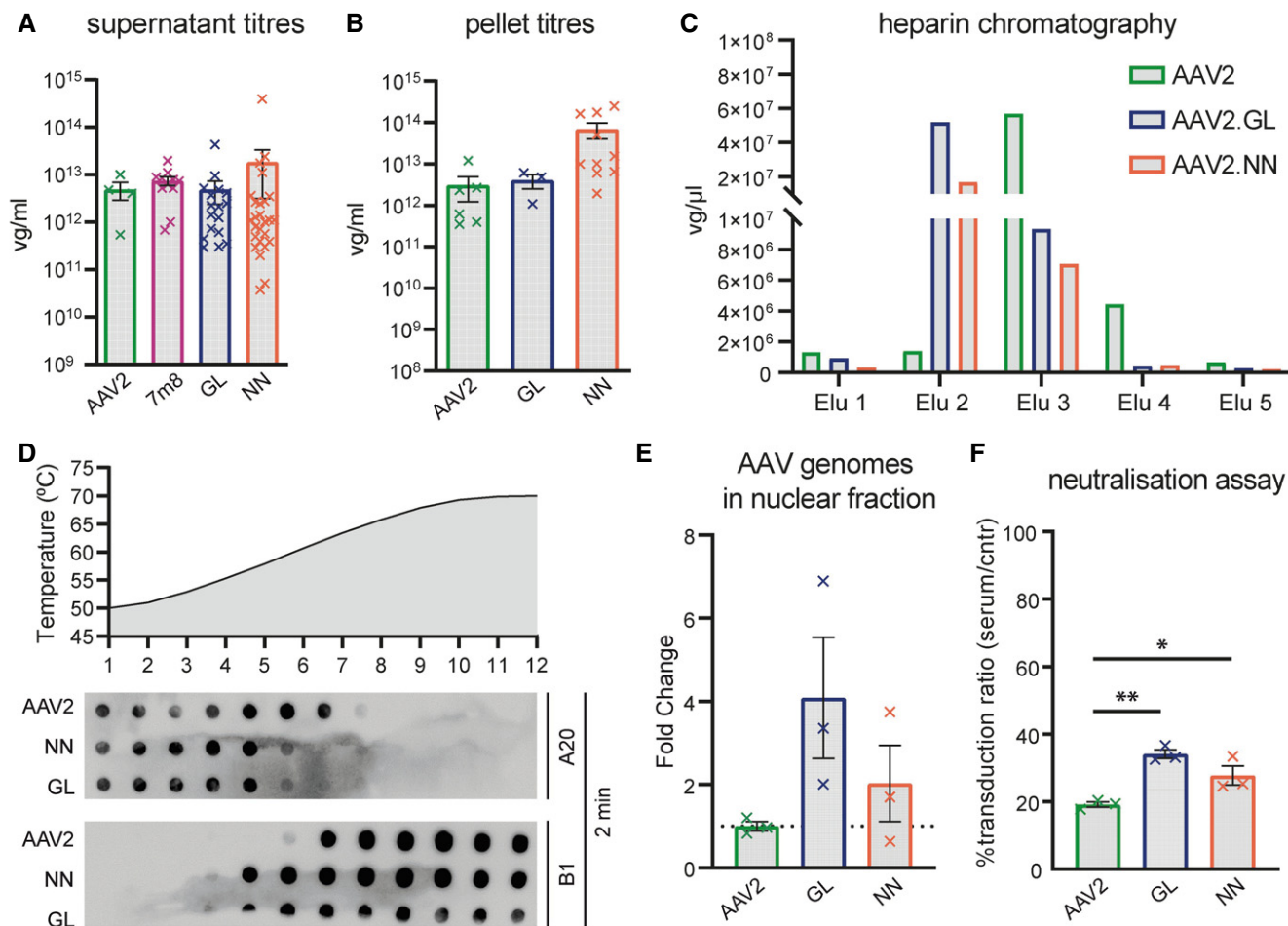


**Figure EV3. In vitro characterisation of AAV2.GL and AAV2.NN.**

- A** Production yield of capsids AAV2.GL, AAV2.NN, AAV2 and AAV2.7m8 quantified by qPCR as viral genomes (vg)/ml, harvested from HEK293T supernatant during standard AAV production. Biological replicates AAV2  $n = 4$ , AAV2.7m8  $n = 11$ , AAV2.GL  $n = 17$ , AAV2.NN  $n = 26$ . Bars show mean  $\pm$  SEM.
- B** Same as for (A) with comparison only to AAV2, harvested from HEK293T cell pellet. Biological replicates AAV2  $n = 6$ , AAV2.GL  $n = 3$ , AAV2.NN  $n = 10$ . Bars show mean  $\pm$  SEM.
- C** Heparin affinity assay performed using chromatography. Consecutive eluates from the heparin column were used to detect the presence of AAV2, AAV2.GL and AAV2.NN, indicating binding strength.
- D** Capsid stability assay comparing AAV2 to AAV2.GL and AAV2.NN. Dot plots of AAV particles stained for A20 and B1, following incubation for 2 min, at consecutive degeneration steps in the form of increasing temperature.
- E** qPCR quantification of rAAV genomes in the nuclear fraction of transduced HeLa cells, normalised to cellular gDNA. Biological replicates  $n = 3$ . Bars show mean  $\pm$  SEM.
- F** Neutralisation assay using HeLa cells after pre-incubating AAV2, AAV2.GL and AAV2.NN with human serum. rAAV vector-induced eGFP signal served as transduction reporter. The % ratio of transduced cells after pre-incubating AAVs with serum relative to control (cntr) unchallenged AAVs is shown. Biological replicates  $n = 3$ . Bars show mean  $\pm$  SEM. One-way ANOVA with Holm–Sidak multiple comparisons test was performed.  $*P \leq 0.05$ ,  $**P \leq 0.01$ . Detailed statistical analysis in Appendix Table S1.

Source data are available online for this figure.

**Figure EV4. Structural modelling of novel capsids.**

Comparative modelling of novel capsid variants (Robetta.bakerlab.org/submit) based on AAV2 (PDB 6IH9) processed using Chimera (Pettersen *et al*, 2004).

- A, B Full capsid of AAV2.GL and AAV2.NN, respectively, with the 7-mer peptide insert in red and the alanine linker in yellow.
- C, D Overlapped structural monomers of AAV2.GL and AAV2.NN, respectively, shown in blue, overlapped to AAV2, shown in white. 7-mer peptide insert is shown in red and the alanine linker in yellow. Key residues N587 and R588 shown in green.
- E, F Focused view on the variable loops 3 and 4 of the comparative overlaps in (C) and (D), respectively. The colour scheme is consistent as before.
- G, H Focused view on the variable loops 3 and 4 of the comparative overlap of structural monomers AAV2.GL and AAV2.NN, respectively, with AAV2.7m8 (PDB 6UOR) (Bennett *et al*, 2020). The colour scheme for AAV2.GL (G) and AAV2.NN (H) is as before. The AAV2.7m8 structural monomer is shown in black, and the peptide displayed on loop 4 is shown in cyan.

Source data are available online for this figure.

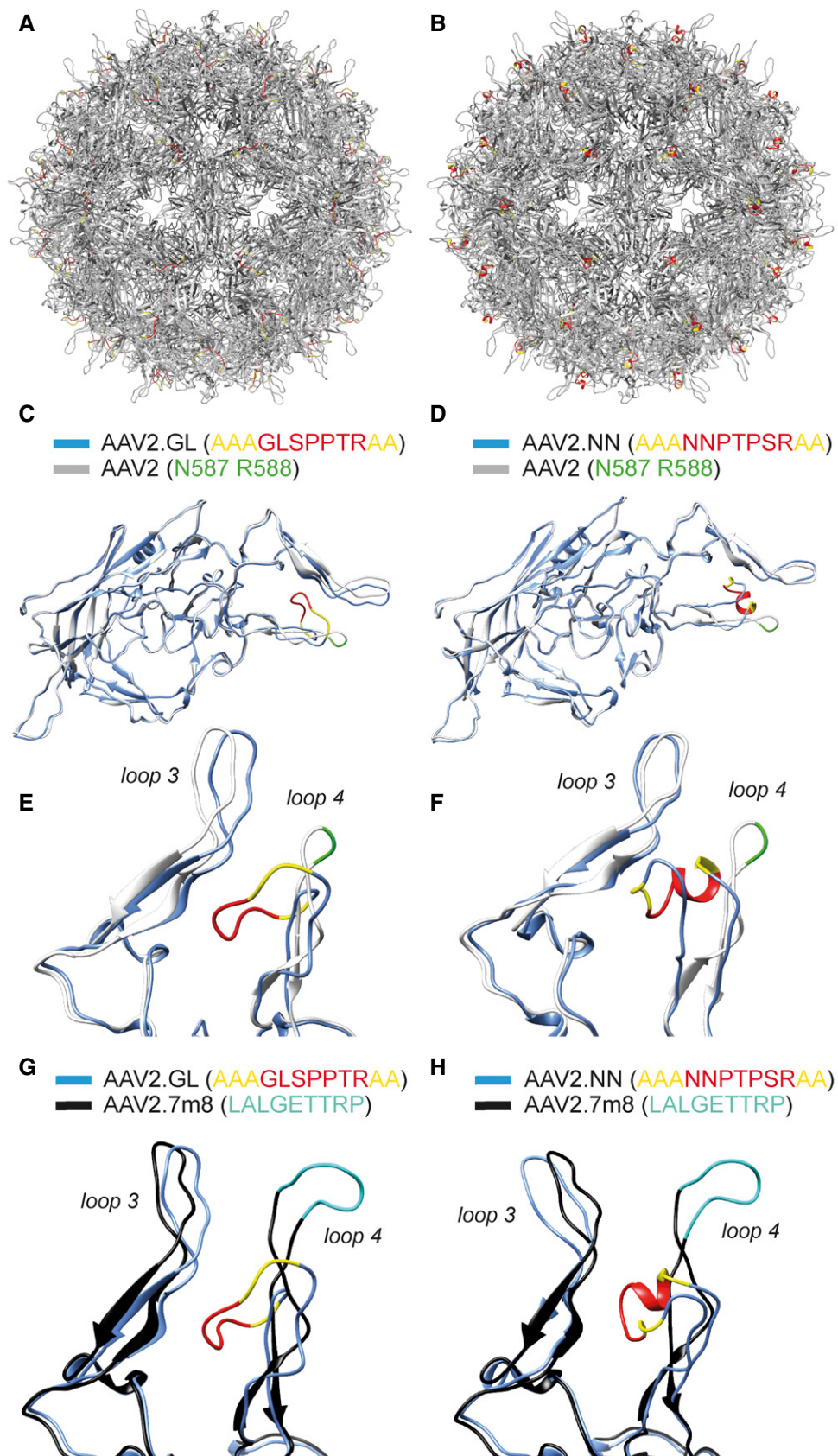
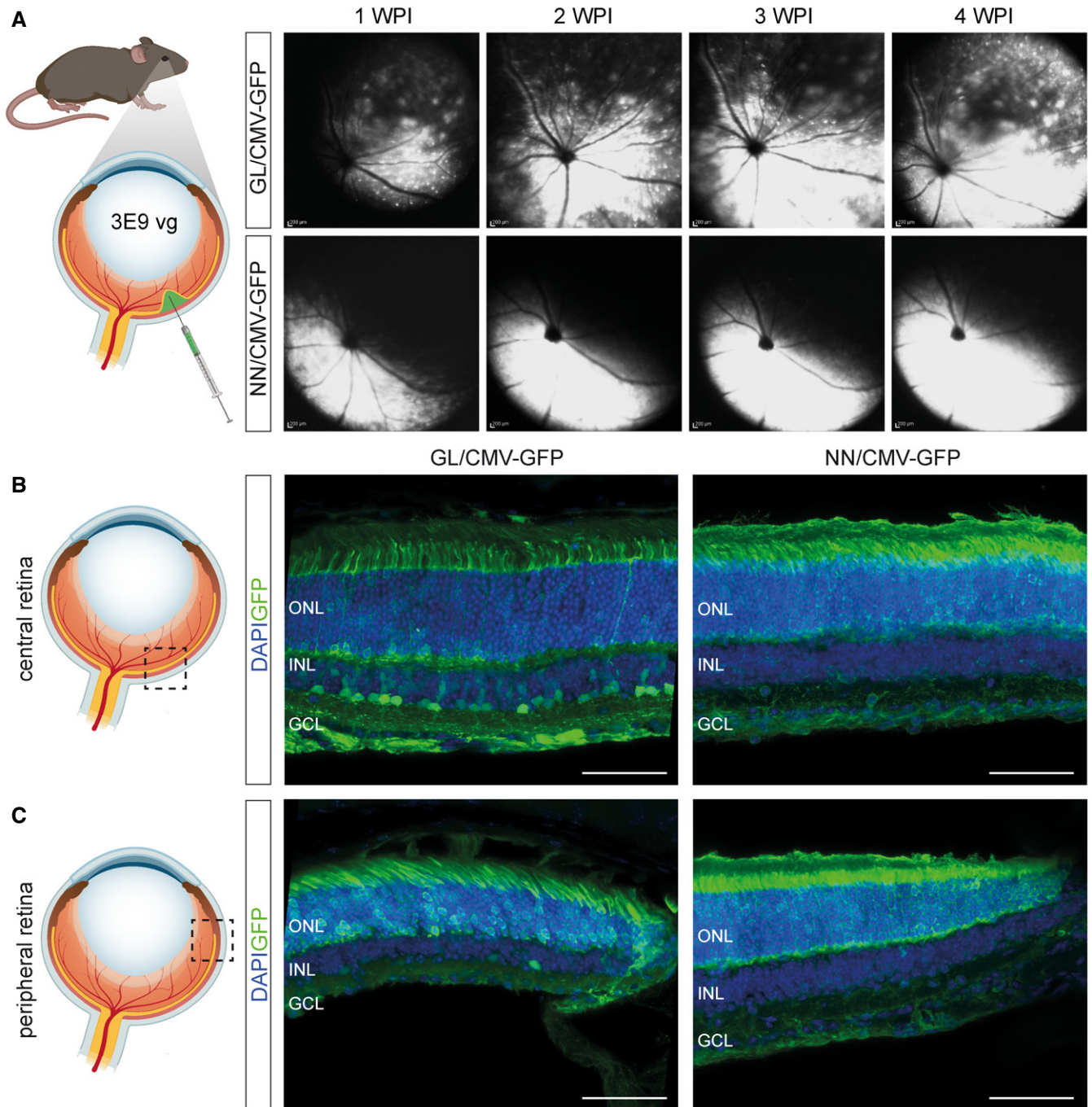


Figure EV4.



**Figure EV5. Subretinal injection of AAV2.GL and AAV2.NN in mouse.**

Vector mediated eGFP expression and lateral spreading after subretinal injection in 1-month-old mouse retinas.

**A** Schematic depiction of subretinal injection in wild-type mice followed by weekly *in vivo* cSLO examinations of the mouse retina from 1 to 4 weeks post-injection (WPI) of 3E9 total vg (in 1  $\mu$ l) of sc-CMV-eGFP packaged with AAV2.GL and AAV2.NN capsid variants.

**B** Schematic depiction of central locus shown in adjacent confocal scans of retinal cross sections immunolabelled for eGFP and DAPI, reporting transduction efficacy of AAV2.GL (left) and AAV2.NN (right).

**C** Schematic depiction of peripheral locus shown in adjacent immunolabelled confocal scans, as in (B).

Data information: Acquisition settings were kept constant for all samples. GFP = eGFP; ONL, outer nuclear layer; INL, inner nuclear layer; GCL, ganglion cell layer. Scale bar: 50  $\mu$ m.

Source data are available online for this figure.